Published in final edited form as:
Sci Signal. 2014 May 20; 7(326): ra46. doi:10.1126/scisignal.2004854.

Reconstituted Human TPC1 Is a Proton-Permeable Ion Channel and Is Activated by NAADP or Ca^{2+}

Samantha J. Pitt[1], **Andy K. M. Lam**[2], **Katja Rietdorf**[2], **Antony Galione**[2], **Rebecca Sitsapesan**[2]

[1]School of Medicine, University of St Andrews, St Andrews KY16 9TF, UK

[2]Department of Pharmacology, University of Oxford, Mansfield Road, Oxford, OX1 3QT, UK

Abstract

NAADP potently triggers Ca^{2+} release from acidic lysosomal and endolysosomal Ca^{2+} stores. Human two-pore channels (TPC1 and TPC2), which are located on these stores, are involved in this process but there is controversy over whether TPC1 and TPC2 constitute the Ca^{2+} release channels. We, therefore, examined the single-channel properties of human TPC1 after reconstitution into bilayers of controlled composition. We found TPC1 was permeable not only to Ca^{2+} but also to monovalent cations and that permeability to protons was the highest (relative permeability sequence $H^+ >> K^+ > Na^+ \geq Ca^{2+}$). NAADP or Ca^{2+} activated TPC1 and the presence of one of these ligands was required for channel activation. The endolysosome-located lipid phosphatidylinositol 3,5 bisphosphate, [$PI(3,5)P_2$] had no effect on TPC1 open probability but significantly increased the relative permeability of Na^+ to Ca^{2+} and of H^+ to Ca^{2+}. Furthermore, our data showed that, although both TPC1 and TPC2 are stimulated by NAADP, these channels differ in ion selectivity and modulation by Ca^{2+} and pH. We propose that NAADP triggers H^+ release from lysosomes and endolysosomes through activation of TPC1 but that the Ca^{2+}-releasing ability of TPC1 will depend on the ionic composition of the acidic stores and may be influenced by other regulators that affect TPC1 ion permeation.

Introduction

The potent ability of nicotinic acid adenine dinucleotide phosphate (NAADP) to release Ca^{2+} from acidic lysosomal organelles is a key signaling mechanism by which NAADP initiates or modulates many cellular processes (1–3). However, the identities of the NAADP-binding targets and of the Ca^{2+}-release channels involved are still debated. There is evidence that two-pore channels (TPCs) are required for NAADP-induced Ca^{2+} release from lysosomal Ca^{2+} stores (4–8). Previously, we demonstrated that, when inserted into an

Corresponding author: Rebecca Sitsapesan, rebecca.sitsapesan@pharm.ox.ac.uk, Tel: 01865 271899.

Author contributions: SJP designed the experiments, performed the experiments, analysed the data and contributed towards writing the manuscript. AKML performed the experiments and analysed the data, KR performed the experiments. AG and RS designed the experiments. RS supervised the project and wrote the manuscript. All authors discussed the results and implications and commented on the manuscript at all stages.

Competing interests: The authors declare that they have no competing interests.

Overline: Biophysics

Europe PMC Funders Author Manuscripts

artificial membrane, TPC2 exhibits conductance properties that would enable it to behave as a Ca^{2+}-release channel (9). Furthermore, many of the unique characteristics of NAADP-induced Ca^{2+} release in mammalian cells are reflected in the single-channel gating behavior of TPC2. This includes activation by low concentrations of NAADP (EC_{50}=5 nM), inactivation by high NAADP concentrations, and concentration-dependent activation and inhibition by the synthetic NAADP analog, Ned-19 (9). Other biophysical studies have also provided evidence that NAADP initiates cation fluxes through TPC2 channels, either in experiments in which currents are measured from intact lysosomes or in which single-channel Ca^{2+} currents are monitored after directing TPC2 to the plasma membrane (10, 11).

In animals, TPC2 is predominantly expressed on lysosomes and late endosomes, whereas TPC1 is expressed throughout the endolysosomal system (12, 13). In plants, TPC1 is present on vacuoles and functions as a nonselective cation channel, permeable to Ca^{2+}. The *Arabidopsis* isoform AtTPC1 is activated by cytosolic Ca^{2+}, but there is no evidence that this channel is regulated by NAADP (14). When human TPC1 is overexpressed in human embryonic kidney cells (HEK293) or the human epithelial cell line SKBR3 an increased sensitivity to NAADP is observed with NAADP triggering intracellular Ca^{2+} release at lower concentrations than is required in control cells. (15). In another study, vesicles from the endolysosomal membrane fraction of HEK293 cells overexpressing TPC1 or in which TPC1 was knocked down, were incorporated into bilayers (16). Single-channel currents were recorded with Ba^{2+} as the permeant ion, and NAADP induced an increase in ion channel activity, thus linking NAADP to activation of an ion channel permeable to a divalent cation (16). Two additional reports suggest that TPC1 and TPC2 are not regulated by NAADP but instead are activated by other factors, such as the lipid, phosphatidylinositol 3,5 bisphosphate, [$PI(3,5)P_2$], energy status, or nutrient levels (17, 18). These studies (17, 18) also report that Na^+ currents rather than Ca^{2+}currents are elicited by $PI(3,5)P_2$ in endolysosomes excised from cells overexpressing TPC1 or TPC2.

To characterize ion conduction through TPC1 and the mechanisms regulating TPC1 activity, we purified human, recombinant TPC1 and incorporated the channels into artificial membranes under voltage-clamp conditions. To enable direct comparison with TPC2, we analyzed both TPC1 and TPC2 in this in-vitro system under the same conditions as those previously used to study TPC2 in artificial bilayers (9). We show that regulation of gating and ionic selectivity in TPC1 and TPC2 are different and suggest that these properties will permit TPC1 and TPC2 to perform different physiological roles. In particular, TPC1 is more permeable to protons than K^+, Na^+, or Ca^{2+} and, therefore, is likely to release H^+ from lysosomes and endolysosomes in response to activation by NAADP or Ca^{2+}.

Results

Basic biophysical properties of TPC1

To compare the biophysical characteristics of TPC1 and TPC2 channels, we purified human TPC1 (histidine-tagged) and human TPC2 from HEK293 cells overexpressing either of these proteins (fig. S1A) and incorporated the proteins into artificial membranes under voltage-clamp conditions (Fig. 1A). Vesicles containing TPC1 or TPC2 were added to the *cis* chamber. We consistently found that (i) the voltage-dependence of TPC1 was always similar

[open probability (Po) was increased by positive holding potentials]; (ii) NAADP only activated TPC1 or TPC2 when added to the *cis* chamber but never activated either channel when added to the *trans* chamber; (iii) TPC1 was activated only by *cis* Ca^{2+} and not by *trans* Ca^{2+} and (iv), for TPC1, the effect of *trans* 100 mM HCl always produced currents 10-100 fold greater than those observed in the presence of 100 mM *cis* HCl. We, therefore, considered that the *cis* chamber corresponded to the cytosolic channel side of TPC1 or TPC2 and the *trans* chamber to the intralysosomal (luminal) side. To avoid confusion, we hereafter refer to the *cis* chamber as the "cytosolic" chamber and the *trans* chamber as the "luminal" chamber.

In symmetrical K^+ solutions (see Materials and Methods for compositions of each ionic solution), in the presence of NAADP on the cytosolic side, the single channel conductance of TPC1 and TPC2 was different (Fig. 1B): Single-channel conductance was 87 ± 3 pS for TPC1 and 296 ± 6 pS for TPC2. Under these conditions, at a holding potential of +20 mV, the Po of TPC2 [0.04±0.02] was much less than the Po of TPC1 [0.26±0.06]. As a control, we used the same purification protocol to prepare vesicles from HEK293 cells that were not overexpressing TPC proteins and incorporated these membranes into the bilayer. We observed no single-channel currents in the presence or absence of NAADP (fig. S1B). We did not ever observe any 296 pS events with the TPC1 preparations or any 87 pS events with the TPC2 preparations and, therefore, these preparations are internal controls of each other.

To investigate whether TPC1 is also permeable to anions, we examined if the reversal potential (calculated according to the Nernst equation) of the current-voltage (I/V) relationship in nonsymmetrical conditions (luminal 210 mM KCl; cytosolic 510 mM KCl) was shifted towards the reversal potential for Cl^- (Fig. 1C). In this gradient, the reversal potential of the TPC1 I/V relationship was shifted from 0 mV in symmetrical solutions (data from Fig. 1B shown as a dotted line) to -25 ± 2.9 mV. This is close to the predicted reversal potential for K^+ (-22 mV) indicating that TPC1 is impermeable to Cl^-.

The membrane potential across lysosomes and other regions of the endolysosomal system depends on the type of lysosomal structure (19) and can be rapidly altered in response to various cellular stimuli, such as those that trigger Ca^{2+} release. Therefore it is important to understand how TPC1 responds to positive and negative holding potentials. We found that the Po of TPC1 is significantly higher at +20 mV (cytosolic relative to luminal) than at -20 mV (Fig. 1D), suggesting that in cells the channel may be regulated by lysosomal membrane potentials.

The effects of cytosolic NAADP and Ca^{2+} on TPC1 gating

By isolating TPC1 and TPC2 from lysosomal membranes and hence from the possible interaction with other unspecified regulators present in the membrane or within lysosomes, we can investigate the regulatory properties of these ion channels. With this experimental technique and in symmetrical KCl solutions, we have previously demonstrated that TPC2 is activated by cytosolic NAADP (9). In the absence of NAADP, in symmetrical KCl solutions, TPC2 exhibited an extremely low Po (approximating to zero),. These occasional brief openings were not abolished by reducing the cytosolic or luminal free [Ca^{2+}] from 10 μM to 1 nM, suggesting that TPC2 opening is independent of Ca^{2+} and that TPC2 may be

constitutively active (to a very low level) in the absence of activating ligands. Here, we investigated whether the addition of Ca^{2+} (Fig. 2A) or NAADP (Fig. 2B) to the cytosolic side of TPC1 affected the Po of TPC1 when exposed initially to symmetrical solutions of KCl, 10 μM free Ca^{2+}, pH 7.2 (Fig. 2A-C). Single-channel analysis showed that the Po of TPC1 was unchanged by the addition of cytosolic NAADP (Fig. 2B and C). However, reducing the free cytosolic [Ca^{2+}] to <1 nM by the addition of EGTA, eliminated all TPC1 single-channel events and subsequent addition of cytosolic NAADP stimulated channel activation (Fig. 2A and C). NAADP had no effect when added to the luminal chamber (fig S2). Quantification of the mean data from these experiments (Fig. 2C) showed that the Po was not significantly different when TPC1 was activated by NAADP alone or by cytosolic Ca^{2+} alone or in the presence of both, indicating that these two ligands do not have a potentiating effect on channel activity at these concentrations. Thus, Ca^{2+} or NAADP present on the cytosolic side activated TPC1 in the bilayer system; whereas TPC2 is insensitive to cytosolic Ca^{2+} in the range 1 nM – 10 μM (9).

We also investigated the effects of adding high concentrations of cytosolic NAADP (1 mM) or the synthetic NAADP analog Ned-19 (1 μM) to TPC1, because both agents inactivate TPC2 at these concentrations (9). Under identical experimental conditions, using K^+ as the permeant ion (symmetrical KCl solution) and in the presence of 10 μM cytosolic Ca^{2+}, neither cytosolic NAADP (1 mM) nor Ned-19 (1 μM) affected TPC1 activity: The Po was 0.24 ± 0.08 before (n=4) and 0.28 ± 0.09 after addition of cytosolic NAADP (n=4) and was 0.29 ± 0.05 before (n=3) and 0.31 ± 0.04 after the addition of cytosolic Ned-19 (n=3). Thus, pharmacological regulation of TPC1 and TPC2 appears different.

Investigation of Na^+ permeation in TPC1

To understand the potential physiological role of TPC1, we examined the conductance and relative permeability of ions that are relevant for lysosome function, including K^+, Na^+, Ca^{2+}, and H^+. The initial experiments showed that TPC1 is permeable to K^+ (Fig. 1). Using a symmetrical NaCl solution and NAADP (100 nM) in the cytosolic chamber (Fig. 3A), we found that TPC1 conducted Na^+ with a single-channel conductance of 68 ± 3 pS, which is lower than that for K^+ (87 pS) (Table 1). We assessed the relative K^+/Na^+ permeability ratio (P_{K^+}/P_{Na^+}) for TPC1 under conditions in which K^+ is the permeant ion in the luminal chamber and Na^+ is the permeant ion in the cytosolic chamber (210 mM KCl luminal:210 mM NaCl cytosolic) (Fig. 3B). The reversal potential of 12 ± 1.3 mV equates to a P_{K^+}/P_{Na^+} of 1.6 ± 0.08, indicating that, under bi-ionic conditions, K^+ is slightly more permeant than Na^+ (Table 2). With Na^+ as the only permeant ion, Po was much less than with K^+ as permeant ion (Fig. 3C, Table 1).

Investigating Ca^{2+} permeation through TPC1

We have previously shown that the reconstituted TPC2 is more permeable to Ca^{2+} than to K^+, exhibiting a K^+/Ca^{2+} permeability ratio ($P_{K^+}/P_{Ca^{2+}}$) of 0.38, which indicates that Ca^{2+} is ~3 times more permeable than K^+ [9]. This discrimination for Ca^{2+} over K^+ may enable TPC2 to behave as a Ca^{2+}-release channel in cells. To examine whether the reconstituted TPC1 behaves similarly, we investigated the Ca^{2+} permeability of TPC1 using identical recording solutions to those used in experiments with TPC2 (9). When exposed to solutions

in which Ca^{2+} was the only permeant ion (Tris/HEPES: Ca^{2+} glutamate solutions, see Materials and Methods) (Fig. 3D), TPC1 activity was detected and the I/V relationship revealed a single-channel conductance of 19 pS ± 2 pS (Fig. 3D, Table 1), which is similar to the Ca^{2+} conductance of TPC2 (18 pS) (9). To examine the relative K^+/Ca^{2+} permeability of TPC1, we used solutions in which K^+ is the permeant ion in the cytosolic chamber and Ca^{2+} is the permeant ion in the luminal chamber (210 mM KCl cytosolic:210 mM $CaCl_2$ luminal) (Fig. 3E). This yields a K^+/Ca^{2+} permeability ratio ($P_{K^+}/P_{Ca^{2+}}$) of 9 ± 2.4 (Table 2), indicating that TPC1 is substantially more permeable to K^+ than Ca^{2+}. In experiments in which Na^+ replaced K^+ as the permeant ion in the cytosolic chamber (210 mM NaCl cytosolic:210 mM $CaCl_2$ luminal) (Fig. 3F), we calculated a $P_{Na^+}/P_{Ca^{2+}}$ of 1.1 ± 0.11 (Table 2). Thus our data suggested a TPC1 relative permeability sequence of $K^+ > Na^+ \geq Ca^{2+}$.

Regulation of TPC1 function by luminal pH

Lysosomes are more acidic than the cytoplasm and the endoplasmic or sarcoplasmic reticulum (ER/SR), and fluctuations in intralysosomal concentrations of protons are associated with Ca^{2+} release from lysosomes and other lysosomal functions (20–23). To investigate if an acidic environment influences TPC1 function, we incorporated TPC1 into bilayers and recorded in symmetrical solutions of 210 mM K^+-acetate. We used noise analysis to monitor the effects of changing $[H^+]$, because in acidic solutions single-channel openings and closings were too rapid to accurately measure. When luminal pH was reduced from 7.2 to 4.8, we observed an increase in TPC1 mean current at the holding potential of -20 mV (Fig. 4A). The increased current appeared to result from an increase in TPC1 Po, but, because of the difficulty in resolving the brief gating events, we cannot rule out that conductance was also altered.

In symmetrical solutions of 210 mM K^+-acetate at pH 7.2, the reversal potential is 0 mV. However, changing luminal pH to 4.8 resulted in positive current flowing in the luminal to cytosolic direction (Fig. 4B). Because [acetate] and $[K^+]$ are symmetrical and because H^+ is the only possible permeant ion, H^+ flowing in the luminal to cytosolic direction must be responsible for the detected current (Fig. 4B). To examine the H+ permeability of TPC1 in more detail, we used solutions similar to those used for measuring H^+ currents through proton channels (24, 25). The solutions contain only HCl so that H^+ can be the only permeant ion. We found that, as expected, in symmetrical 10 mM HCl (pH 2), the reversal potential was 0 mV (Fig. 4C). With 10 mM luminal HCl (pH 2) and 100 mM cytosolic HCl (pH 1), the reversal potential was -47 ± 4 mV (Fig. 4D); whereas with 10 mM cytosolic HCl (pH 2) and 100 mM luminal HCl (pH 1), the reversal potential was +43 ± 6 mV (Fig. 4E). Both values correspond closely to the calculated H^+ equilibrium potential and are far from the Cl^- equilibrium potential in each case, consistent with TPC1 being permeable to protons and impermeable to anions.

To predict whether TPC1 could conduct protons in cells, we assessed the relative permeability of protons to other cations using bi-ionic conditions with either 210 mM KCl, NaCl, or $CaCl_2$ in the cytosolic chamber and 10 mM HCl (pH 2) in the luminal chamber (fig. S3) and calculated the relative permeabilities (Table 2). These data indicated that TPC1

is ~39-fold more selective for H^+ than for K^+, 67-fold more selective for H^+ than for Na^+ and 500-fold more selective for H^+ than for Ca^{2+}.

Effect of luminal [Ca^{2+}] on TPC1 gating

Not only was TPC1 permeable to H^+ but the Po was also increased at lower luminal pH (Fig 4A), suggesting that channel gating could be affected by changes in endolysosomal and lysosomal pH in cells. We have previously shown that TPC2 activity is increased in the presence of high [Ca^{2+}] on the luminal side (9). To determine if increasing [Ca^{2+}] on the luminal side affected TPC1 activity, we used symmetrical KCl solution and recorded Po at +20 mV. Increasing luminal Ca^{2+} from 10 μM to 500 μM (Fig. 5A andB), the latter of which is the likely [Ca^{2+}] in lysosomes, did not affect Po. In the presence of 500 μM luminal Ca^{2+}, the addition of 200 nM NAADP to the cytosolic side also did not significantly change Po (Fig. 5C and D).

Effects of phosphatidylinositol 3,5-bisphosphate on TPC1 function

Some reports suggest that TPCs are not regulated by NAADP but are activated by $PI(3,5)P_2$ (17, 18). In isolated lysosomal organelles, increased Na^+ currents were detected after the addition of cytosolic $PI(3,5)P_2$ (18). We, therefore, investigated if $PI(3,5)P_2$ activated TPC1 with Na^+ as the permeant ion (Fig. 6). The experiments were conducted at +30 mV because of the very low Po and single-channel conductance in these experimental conditions. To determine if the addition of $PI(3,5)P_2$ to the cytosolic side triggered Ca^{2+}-independent TPC1 activity [as we observed with NAADP (Fig. 2)], we lowered cytosolic [Ca^{2+}] to subactivating concentrations with EGTA before adding $PI(3,5)P_2$. We observed no activation by $PI(3,5)P_2$ at identical concentrations to those used previously (17, 18). Subsequent addition of NAADP stimulated TPC1 channel activity, demonstrating that the channel was present and responsive to other ligands (Fig. 6A,B). To determine if $PI(3,5)P_2$ potentiated the effect of NAADP, we measured single-channel activity when NAADP was added before (Fig. 6C) or after (Fig. 6B) addition of $PI(3,5)P_2$ to the cytosolic chamber. Po was similar under both conditions. In the presence of Ca^{2+} on the cytosolic side, Po was also unchanged by the addition of 1 μM $PI(3,5)P_2$ to either the cytosolic or luminal side or by the addition of a higher concentration of $PI(3,5)P_2$ to the cytosolic chamber (10 μM) (fig. S4A,B).

We then investigated whether $PI(3,5)P_2$ affected ion permeation through TPC1 by calculating $P_{Na^+}/P_{Ca^{2+}}$ and $P_{H^+}/P_{Ca^{2+}}$ from average currents detected in the presence of 1 μM $PI(3,5)P_2$ (Fig. 6D, E). The reversal potentials were significantly shifted by $PI(3,5)P_2$ in both cases, increasing both the relative permeability to Na^+ and H^+ (Table 2). Thus, in the presence of $PI(3,5)P_2$, TPC1 was more permeable to Na^+ and H^+ than to Ca^{2+}.

Discussion

Our data showed that, when reconstituted into planar phospholipid bilayers, human TPC1 is an ion channel permeable to protons, with a relative permeability sequence for cations in the order $H^+ >> K^+ > Na^+ \geq Ca^{2+}$. In this system, we also found that low concentrations of NAADP and Ca^{2+} activated TPC1, increasing Po. In contrast, $PI(3,5)P_2$ did not stimulate channel

opening; $PI(3,5)P_2$ altered the conducting properties of TPC1 by increasing the permeability of H^+ and Na^+ relative to Ca^{2+}.

Comparing the biophysical properties of reconstituted TPC1 and TPC2 channels reveals many similarities. Both are cation channels that are impermeable to anions but permeable to a range of monovalent and divalent cations (9), and both are activated by low concentrations of NAADP. However, there are also differences that are likely physiologically important. For example, whereas TPC2 is more permeable to divalent cations than to monovalent cations, TPC1 exhibited the opposite behavior. This biophysical difference suggests that TPC2 functions as a Ca^{2+}-release channel in cells. In contrast, on the basis of the relative permeabilities of TPC1 for certain cations, we predict that Ca^{2+} represents only a small portion of the ionic flux through TPC1 although this will depend on intralysosomal pH and on intralysosomal Ca^{2+}, Na^+, and K^+ concentrations. Our data also indicated that signals that produce increased $PI(3,5)P_2$ would tend to increase the proportion of Na^+ and H^+ flux relative to Ca^{2+} flux through TPC1 in response to increased NAADP or Ca^{2+} in the cytosol.

Because of the variable estimates of the intraluminal Ca^{2+}, Na^+, and K^+ concentrations within these acidic stores and because the concentrations of ions varies from lysosomes to early and late endosomes (18, 19), we cannot precisely calculate the proton or Ca^{2+} fluxes that will flow from acidic stores through activated TPC1 or TPC2. The resting membrane potential across acidic stores is likely to be positive with respect to the cytosol, ~ +10 to +40 mV depending on the organelle (19, 26). Estimates of the intraluminal $[Ca^{2+}]$ within acidic stores range from 200-600 μM in lysosomes (19, 27) to 3-37 μM in late endosomes (19, 28). Reports for intraluminal Na^+ concentrations range from 20-150 mM and for intraluminal K^+ concentrations range from 20-107 mM (18, 19, 29). The pH inside lysosomes is approximately 4.8 but endosomes are less acidic (19, 30). Although TPC1 is approximately 40-70 times more permeable to H^+ than to K^+ or Na^+, the concentration of H^+ both inside and outside lysosomal stores is at least ten thousand-fold lower than the concentration of Na^+ or K^+ in either compartment. Therefore, assuming intralysosomal Na^+ is 145 mM (18), activated TPC1 will preferentially flux Na^+ out and K^+ in until the reversal potential (E_{rev}) for Na^+ and K^+ is approached and outward H^+ flux will occur together with a very small flux of Ca^{2+}. Because reconstituted TPC2 is more permeable to Ca^{2+} than to K^+ (9), in response to NAADP, TPC2 may release more Ca^{2+} from lysosomes than is released through TPC1. Alkalinization of endolysosomal compartmentsis associated with NAADP signaling both in sea urchin eggs (21, 31) and in mammalian HeLa cell lines overexpressing TPC2 (32). Our results showing that TPC1 is permeable to protons provides one mechanistic explanation for why NAADP-mediated Ca^{2+} release is associated with alkalinization of acidic stores.

Immunolocalisation studies indicate that the abundance of TPC2 is highest in lysosomes and lower in endosomes; whereas TPC1 is more abundant in endosomes (13). We, therefore, suggest that in the lysosome, TPC2 acts as the primary Ca^{2+}-release pathway with negligible contribution from TPC1. In the less acidic endosomes, with greater amounts of TPC1 than TPC2 and lower concentrations of H^+ compared with lysosomes, TPC1 may have a larger contribution to Ca^{2+} release. This may explain the reports that TPC1 mediates Ca^{2+} release

in studies in which TPC1 is overexpressed to levels exceeding physiological norms or when TPC2 is genetically knocked out (4) or knocked down (15).

We found that TPC1 was inactive in the absence of NAADP and cytosolic Ca^{2+}, and hence appears dependent on ligand activation from the cytosolic side. Without NAADP or activating concentrations of cytosolic Ca^{2+}, TPC1 was inactive irrespective of changes within the luminal compartment such as, voltage, permeant ion, or Ca^{2+}. However, in the presence of activating ligands, we identified other modulators of TPC1 behavior. The Po of TPC1 was much lower in solutions of Na^+ then in solutions of K^+. This modulation of gating by the permeant ion may be due to the binding of the monovalent cation within the conduction pathway or be due to an interaction at sites on the cytosolic or luminal face of the channel. The gating of other channels, are known to be sensitive to the concentration and species of permeant ion (33–37). Thus, in cells, TPC1 activity may largely depend on the ratio of $[K^+]$ to $[Na^+]$ inside acidic stores, which could introduce time dependence to TPC1 fluxes. Assuming that resting intralysosomal $[Na^+]$ is 145 mM (18) and $[K^+]$ is 20 mM, then following the binding of NAADP to TPC1, the Po of the channel may be very low until intraluminal $[Na^+]$ is reduced.

TPC1 Po is significantly lower at holding potentials where the luminal side of the channel is positive with respect to the cytosolic side. In cells, therefore, TPC1 Po may increase as lysosomal membrane potential moves towards 0 mV as Na^+, H^+ and Ca^{2+} are released. Luminal pH also appears to be a key regulator of TPC1 gating and our results indicated that acidic pH could override inhibitory influence of membrane potential. Thus, we predict that the more acidic the compartment, the higher the Po of TPC1 will be in response to activating ligands.

Our findings that the ion conduction and gating properties of TPC1 and TPC2 are different were not surprising given their differences in primary sequence; TPC1 and TPC2 exhibit ~20% sequence identity (6, 7). This divergence enables a flexible flexible Ca^{2+}-release system within acidic organelles since TPC1 and TPC2 can be differentially activated/modulated and can release H^+ and/or Ca^{2+} to a different extent. Although the reconstituted TPC1 and TPC2 channels (9) are both activated by NAADP, TPC1 is also stimulated by cytosolic Ca^{2+}; whereas we have found no evidence that TPC2 activity is regulated by cytosolic Ca^{2+} (38). In cells, this difference will enable increases in cytosolic Ca^{2+} to selectively open populations of TPC1 without opening TPC2 channels. We found that neither cytosolic Ca^{2+} alone nor cytosolic NAADP alone fully activated TPC1 (to Po = 1) and that the simultaneous presence of both ligands did not produce an increase above the maximum Po observed with either ligand alone. This may explain why NAADP-induced currents are not detected in experiments in which high levels of TPC1 are present (18): Micromolar concentrations of Ca^{2+} would be expected to activate TPC1 to a level at which the addition of NAADP would produce no further effect. Perhaps a parallel situation occurs with the plant TPC1 protein, *Arabidopsis* (AtTPC1), which is located on plant vacuoles. AtTPC1 shows some functional similarities to reconstituted purified human TPC1. AtTPC1 is permeable to both monovalent and divalent cations but is impermeable to anions (14, 39). AtTPC1 is activated by cytosolic Ca^{2+} and regulated by voltage (39, 40). There are no

reports that NAADP can activate AtTPC1 but perhaps the sensitivity of the channel to cytosolic [Ca^{2+}] has concealed any activating potential of NAADP.

We did not find any evidence that PI(3,5)P_2 can directly activate TPC1; however, we found that PI(3,5)P_2 shifted the relative permeability of TPC1 in favor of Na^+ and H^+ over Ca^{2+} and, therefore, would be expected to increase Na^+ efflux from lysosomes with activated TPC1. The mechanism for PI(3,5)P_2-mediated modification of ion conduction by TPC1 is unclear. We found that activation of purified, recombinant TPC1 or TPC2 (9) by NAADP is robust. Our data obtained with isolated channels in reconstituted bilayers suggests that the binding sites for NAADP must either be on the channels themselves or on tightly-associated proteins, which is consistent with the work of other groups who monitored TPC1 and TPC2 function in a cellular or lysosomal setting and linked activation of TPC1 and TPC2 directly to the addition of NAADP (4, 7, 12, 41–43). It is surprising that Wang *et al.* (18) could not observe any response to NAADP in patch-clamp experiments with endolysosome-like organelles. However, under certain experimental conditions, NAADP sensitivity may be lost or masked. For example, TPC1 responsiveness to NAADP could be inhibited by high lysosomal [Na^+] or masked by cytosolic Ca^{2+}. The ability of TPC1 to respond to NAADP depends on the N-terminus, because Churamani *et al.* (44) find that NAADP-induced currents are abolished by the introduction of a fluorescent tag onto the N-terminus of TPC1. Additionally, lysosomal membranes contain many other ion channels and proteins that could be regulated by PI(3,5)P_2 and that could indirectly modulate TPC function (45–47). Other groups have detected NAADP-activated currents across lysosomes in patch-clamp studies in cells overexpressing TPC2 (11, 48).

Our study demonstrated that the regulation of TPC1 activity is complex and indicated that the physiological role of TPC1 could vary with location. It is difficult, therefore, to provide a single picture of the exact ionic fluxes that are likely to flow through TPC1 and that are accurate for each organelle in which TPC1 is present. We can, however, provide a simplified overview of the ions that we predict will flow through TPC1 and TPC2 given either an increase in NAADP or an increase in cytosolic [Ca^{2+}] (Fig. 7).

If NAADP increases without a concomitant increase in cytosolic [Ca^{2+}] (1), then both TPC1 and TPC2 will be activated. Na^+ will flow out and K^+ will flow into the acidic Ca^{2+} stores until the relevant reversal potentials are achieved. Ca^{2+} will also flow outwards, primarily through TPC2, as will protons through TPC1. The flux of Ca^{2+} into the cytosol may sufficiently increase the local [Ca^{2+}] to amounts that can prolong the opening of TPC1 but this will depend on the rate of diffusion away from release sites (Fig. 7A). Our experiments showed that TPC1 is more open at +20 mV than at -20 mV (cytosolic with respect to luminal) and this voltage sensitivity of TPC1 may be an important factor in controlling the relative activity of TPC1 and TPC2. When TPC1 or TPC2 or both channels are activated, positive charge carried by Na^+, H^+, and Ca^{2+} will flow out of acidic stores, making the lumen less positive with respect to the cytosol. Under these conditions one would expect TPC1 to become more active. If there is only an increase in cytosolic [Ca^{2+}] (Fig. 7B), then only TPC1 will be activated. Again, Na^+ will flow out and K^+ will flow into the acidic stores at rates that depend on the initial membrane potential and concentrations of intraluminal Na^+ and K^+. Only a trickle of Ca^{2+} will be released, because the main Ca^{2+}-release channel

(TPC2) of acidic Ca^{2+} stores has not been activated. Proton release may become substantial as K^+ and Na^+ equilibrate across the lysosomal membranes (Fig. 7B). It is interesting to speculate that Ca^{2+}-induced H^+ release through TPC1 may be a physiologically relevant signaling pathway.

We conclude by emphasizing that, although TPC1 and TPC2 share certain functional similarities, there are important differences in their ion selectivity and regulation of gating. We suggest that TPC2 acts as the main Ca^{2+}-release channel in lysosomes; whereas TPC1 will release protons, an effect that will, in turn, stimulate the increased opening of TPC2 if they are present on the same organelle (9).

Materials and Methods

Purification of hTPC1

Non-transfected HEK293 cells (WT) and HEK293 cells stably expressing His-tagged human TPC1 (hTPC1.HIS) were resuspended in ice cold IP buffer (150 mM NaCl, 25 mM TRIS, pH 7.4) supplemented with 1x EDTA-free Complete protease inhibitor (Roche). Resuspended cells were then mixed with glass beads (Sigma) at 1:1 v/v ratio, and were homogenized on ice by passing the cells 20 times through a 23 G needle. Nuclei were removed by centrifugation at 2,000 x g for 5 min at 4 °C. The postnuclear supernatants were centrifuged at 100,000 x g for 1 hr at 4 °C to obtain the membrane fractions, which were then solubilized in IP buffer containing 1 % CHAPS overnight at 4 °C. Insoluble material was removed by centrifugation at 14,000 x g for 10 min at 4 °C. His-tagged proteins were isolated from the solubilized membrane fractions using the HisPurTM Cobalt Purification Kit (Pierce). Buffers involved in the purification procedure were all supplemented with 1% CHAPS. hTPC2 was prepared following previously published methods (9).

Western blotting

Protein samples were prepared in 1x laemmli buffer/4% beta-mercaptoethanol but were not heated to prevent heat-induced aggregation. Insoluble material was removed by centrifugation at 14,000 x g for 3 minutes at room temperature prior to gel loading. Proteins were resolved in a NuSep NG 8% precast SDS-PAGE gel in 1x running buffer (25 mM Tris, 192 mM glycine, 0.1% SDS, pH 8.5) at 150 V, which were then wet transferred onto a PVDF-FL membrane (Immobilon) in buffer (48 mM Tris, 39 mM glycine, 0.0375 % SDS, 20 % methanol) at 400 mA for 1hr. The membrane was blocked in Odyssey blocking buffer (Licor) supplemented with 0.1 % Tween 20 for 2 hrs at room temperature and was subsequently incubated overnight at 4°C in 1:1000 polyclonal antibody against HIS (rabbit polyclonal, Pierce). After two 10-min washes with PBS supplemented with 0.1% Tween 20, the membrane was incubated in 1:500 AlexaFluor 633-conjugated goat anti-rabbit IgG (Invitrogen) at room temperature for 1 hr, washed twice with PBS/0.1% Tween 20, and then visualized using the Typhoon scanner (GE Healthcare). A 633 nm laser was used for excitation and the emitted light was bandpass filtered at 670 nm/BP 30. Pixel size was 50 μm.

Single-channel recording and analysis

Purified human TPC1 and TPC2 were incorporated into planar phosphatidylethanolamine lipid bilayers under voltage-clamp conditions using previously described techniques (9, 49) Vesicles were added to the *cis* chamber. The *trans* chamber was held at 0 mV and the *cis* chamber was voltage-clamped at various potentials relative to ground. Fusion of vesicles to the bilayer appeared to deliver channels into the bilayer in a consistent orientation such that the *cis* chamber corresponded to the cytosolic side of TPC1 and TPC2 (Fig. 1A). Single-channel events were recorded in the following solutions:

For experiments in which Ca^{2+} is the permeant ion: Tris/HEPES:Ca^{2+}glutamate solutions contained 250 mM HEPES, 80 mM Tris, 10 μM free Ca^{2+}; pH 7.2 *cis*; 250 mM glutamic acid, 10 mM HEPES, pH 7.2 with $Ca(OH)_2$ giving a free [Ca^{2+}] of 50 mM t*rans*.

For bi-ionic studies: $CaCl_2$ solution contained 210 mM $CaCl_2$, 10 mM HEPES, pH 7.2. For experiments in which K^+ is the permeant ion: Symmetrical 210 mM KCl solutioncontained 210 mM KCl, 10 mM HEPES, 10 μM free Ca^{2+}, pH 7.2 in both *cis* and *trans* chambers.

For experiments in which Na^+ is the permeant ion: Symmetrical 210 mM NaCl solution contained 210 mM NaCl, 10 mM HEPES, 10 μM free Ca^{2+}, pH 7.2 in both *cis* and *trans* chambers.

For experiments in which H^+ is the permeant ion: HCl solutions contained HCl at either 10 mM or 100 mM in the *cis* or *trans* chambers.

For experiments in which the effects of pH were investigated: K^+-acetate solution contained symmetrical 210 mM K^+ acetate, 10 mM HEPES, 10 μM free [Ca^{2+}] and pH of *cis* and *trans* chamber varied between 7.2 or 4.8.

The free [Ca^{2+}] and pH of the solutions were determined using a Ca^{2+} electrode (Orion 93-20) and a Ross-type pH electrode (Orion 81-55) as described previously (49). The approximate free [Ca^{2+}] following addition of 10 mM EGTA to the *cis* chamber, was calculated as <1nM using the MaxChelator program (www.standford.edu/~cpatton/maxc.html).

Current recordings were monitored under voltage-clamp conditions using a BC-525C amplifier (Warner Instruments, CT). Channel recordings were low-pass filtered at 10 kHz with a 4-pole Bessel filter, sampled at 100 kHz using an ITC-18 data acquisition interface (HEKA Elektronik) and recorded onto the computer hard drive using WinEDR 3.05 acquisition software (John Dempster, University of Strathclyde). The recordings were subsequently filtered at 800 Hz (-3 dB) using the low pass digital filter within WinEDR 3.05. Measurements of single-channel current amplitudes were made using WinEDR. The closed and fully open current levels were assessed manually using cursors.

Unless otherwise stated, channel open probability (Po) was calculated over 3 min of continuous recording using TACfit 4.2.0 software. Channel openings were detected by the 50 % threshold method (50). Only experiments where ≤ 4 channels were gating in the bilayer were used for Po analysis. TPC1 Po was always increased by positive holding

potentials with monovalent cations as permeant ions. The voltage dependency of TPC1 enabled us to ascertain the number of channels within the bilayer by briefly applying a holding command of +60 mV. Po was calculated using the following equation.

$$Po = \frac{[Popen1 + 2(Popen2) + \ldots\ldots n(PopenN)}{N}$$

Where *Popen*1 is the probability of one channel opening and *Popen*2 is the probability of two channels being open simultaneously. N is the number of channels in the bilayer.

Predicted reversal potentials were calculated using the Nernst equation. The permeability ratio when comparing monovalent cations to K^+ was calculated from the Goldman-Hodgkin-Katz equation (51):

$$P_x/P_y = [Y^+]/[X^+] \cdot \exp(-E_{rev}F/RT)$$

where R is the ideal gas constant (8.314 J mol^{-1}), T is the temperature in kelvin, z is the valency of the ion and F is the Faraday constant (9.6485 x 10^4 C mol^{-1}). The relative Ca^{2+} to monovalent (K^+ or Na^+) permeability ratio (P_{Ca}^{2+}/P_x^+) was calculated using the Fatt-Ginsborg equation (52):

$$P_x/P_y = [Y^+]/4[X^{2+}] \cdot \exp(E_{rev}F/RT) \cdot [\exp(E_{rev}F/RT + 1]$$

E_{rev} is the zero current reversal potential. The reversal potential was taken to be the point at which current fluctuations were at a minimum. Junction potentials were calculated using Clampex software version 10.2 (Molecular Devices, Sunnyvale, CA) and subtracted from the reversal potential obtained from each measurement.

Noise analysis was performed with WinEDR version 3.05. The current fluctuations across the bilayer were subdivided into multiple segments in time with each segment containing *N* samples. The mean current for each segment was plotted as a function of time and was computed by the formula:

$$I_{mean} = \frac{\sum_{i=1}^{N} I(i)}{N}$$

where *I(i)* is the amplitude of the *i*th current and *N* is the number of samples in the segment. Mean current measurements were obtained with multiple channels incorporated into the bilayer at the various holding potentials and was measured over ≥ 1min. The mean data from multiple experiments were then calculated and plotted as a function of voltage.

Statistics

Data were expressed as mean ± SEM. Where appropriate, a Student's *t*-test was used to assess the difference between mean values. Where multiple treatments were compared, ANOVA followed by a modified *t*-test was used to assess the difference between treatments. A p value of <0.05 was taken as significant.

Materials

NAADP was made in-house according to previously established methods (53). A stock solution of NAADP was made in de-ionized water. Dic8 PI(3,5)P_2 abbreviated to (PI(3,5)P_2) was obtained from Tebu-Biol Ltd (Peterborough, UK) and stored in de-ionized water. Other chemicals were AnalaR or the best equivalent grade from BDH (Poole, UK) or Sigma-Aldrich (Dorset, UK). All solutions were made in de-ionized water and those for use in bilayer experiments were filtered through a Millipore membrane filter (0.45-μm pore).

Supplementary Material

Refer to Web version on PubMed Central for supplementary material.

Acknowledgements

We thank Miss F. O'brien and Dr E. Venturi for their thoughtful comments on the manuscript.

Funding: This work was supported by the BHF (RS) and Wellcome Trust (AG). AG and RS are BHF CRE Principal Investigators. SJP is a Royal Society of Edinburgh Biomedical Research Fellow. The funders had no role in study design, data collection and analysis, decision to publish, or preparation of the manuscript.

References

1. Churchill GC, Okada Y, Thomas JM, Genazzani AA, Patel S, Galione A. NAADP mobilizes Ca^{2+} from reserve granules, lysosome-related organelles, in sea urchin eggs. Cell. 2002; 111:703–708. [PubMed: 12464181]
2. Guse AH, Lee HC. NAADP: A Universal Ca^{2+} Trigger. Sci Signal. 2008; 1
3. Galione A, Morgan AJ, Arredouani A, Davis LC, Rietdorf K, Ruas M, Parrington J. NAADP as an intracellular messenger regulating lysosomal calcium-release channels. Biochem Soc Trans. 2010; 38:1424–1431. [PubMed: 21118101]
4. Calcraft PJ, Ruas M, Pan Z, Cheng XT, Arredouani A, Hao XM, Tang JS, Rietdorf K, Teboul L, Chuang KT, Lin PH, et al. NAADP mobilizes calcium from acidic organelles through two-pore channels. Nature. 2009; 459:596–600. [PubMed: 19387438]
5. Galione A, Evans AM, Ma JJ, Parrington J, Arredouani A, Cheng XT, Zhu MX. The acid test: the discovery of two-pore channels (TPCs) as NAADP-gated endolysosomal Ca^{2+} release channels. Pflugers Archiv. 2009; 458:869–876. [PubMed: 19475418]
6. Zhu MX, Ma J, Parrington J, Galione A, Evans AM. TPCs: Endolysosomal channels for Ca^{2+} mobilization from acidic organelles triggered by NAADP. FEBS Lett. 2010; 584:1966–1974. [PubMed: 20159015]
7. Zong XG, Schieder M, Cuny H, Fenske S, Gruner C, Rotzer K, Griesbeck O, Harz H, Biel M, Wahl-Schott C. The two-pore channel TPCN2 mediates NAADP-dependent Ca^{2+}-release from lysosomal stores. Pflugers Archiv. 2009; 458:891–899. [PubMed: 19557428]
8. Brailoiu E, Hooper R, Cai X, Brailoiu GC, Keebler MV, Dun NJ, Marchant JS, Patel S. An Ancestral Deuterostome Family of Two-pore Channels Mediates Nicotinic Acid Adenine Dinucleotide Phosphate-dependent Calcium Release from Acidic Organelles. J Biol Chem. 2010; 285:2897–2901. [PubMed: 19940116]

9. Pitt SJ, Funnell TM, Sitsapesan M, Venturi E, Rietdorf K, Ruas M, Ganesan A, Gosain R, Churchill GC, Zhu MX, Parrington J, et al. TPC2 is a novel NAADP-sensitive Ca^{2+} release channel, operating as a dual sensor of luminal pH and Ca^{2+} J Biol Chem. 2010; 285:35039–35046. [PubMed: 20720007]
10. Brailoiu E, Rahman T, Churamani D, Prole DL, Brailoiu GC, Hooper R, Taylor CW, Patel S. An NAADP-gated two-pore channel targeted to the plasma membrane uncouples triggering from amplifying Ca^{2+} signals. J Biol Chem. 2010; 285:38511–38516. [PubMed: 20880839]
11. Schieder M, Roetzer K, Brueggemann A, Biel M, Wahl-Schott CA. Characterization of Two-pore Channel 2 (TPCN2)-mediated Ca^{2+} Currents in Isolated Lysosomes. J Biol Chem. 2010; 285:21219–21222. [PubMed: 20495006]
12. Zhu MX, Evans AM, Ma J, Parrington J, Galione A. Two-pore channels for integrative Ca signaling. Commun Integr Biol. 2010; 3:12–17. [PubMed: 20539775]
13. Zhu MX, Ma J, Parrington J, Calcraft PJ, Galione A, Evans AM. Calcium signaling via two-pore channels: local or global, that is the question. Am J Physiol Cell Physiol. 2010; 298:C430–441. [PubMed: 20018950]
14. Hedrich R, Marten I. TPC1 – SV Channels Gain Shape. Mol Plant. 2011; 4:428–441. [PubMed: 21459829]
15. Brailoiu E, Churamani D, Cai XJ, Schrlau MG, Brailoiu GC, Gao X, Hooper R, Boulware MJ, Dun NJ, Marchant JS, Patel S. Essential requirement for two-pore channel 1 in NAADP-mediated calcium signaling. J Cell Biol. 2009; 186:201–209. [PubMed: 19620632]
16. Rybalchenko V, Ahuja M, Coblentz J, Churamani D, Patel S, Kiselyov K, Muallem S. Membrane Potential Regulates Nicotinic Acid Adenine Dinucleotide Phosphate (NAADP) Dependence of the pH- and Ca^{2+}-sensitive Organellar Two-pore Channel TPC1. J Biol Chem. 2012; 287:20407–20416. [PubMed: 22500018]
17. Cang C, Zhou Y, Navarro B, Seo Y-j, Aranda K, Shi L, Battaglia-Hsu S, Nissim I, Clapham David E, Ren D. mTOR Regulates Lysosomal ATP-Sensitive Two-Pore Na+ Channels to Adapt to Metabolic State. Cell. 2013; 152:778–790. [PubMed: 23394946]
18. Wang X, Zhang X, Dong XP, Samie M, Li X, Cheng X, Goschka A, Shen D, Zhou Y, Harlow J, et al. TPC proteins are phosphoinositide-activated sodium-selective ion channels in endosomes and lysosomes. Cell. 2012; 151:372–383. [PubMed: 23063126]
19. Morgan AJ, Platt FM, Lloyd-Evans E, Galione A. Molecular mechanisms of endolysosomal Ca^{2+} signalling in health and disease. Biochem J. 2011; 439:349–374. [PubMed: 21992097]
20. Morgan AJ. Sea urchin eggs in the acid reign. Cell Calcium. 2011; 50:147–156. [PubMed: 21251713]
21. Morgan AJ, Galione A. NAADP induces pH changes in the lumen of acidic Ca^{2+} stores. Biochem J. 2007; 402:301–310. [PubMed: 17117921]
22. Cosker F, Cheviron N, Yamasaki M, Menteyne A, Lund FE, Moutin MJ, Galione A, Cancela JM. The ecto-enzyme CD38 is a nicotinic acid adenine dinucleotide phosphate (NAADP) synthase that couples receptor activation to Ca^{2+} mobilization from lysosomes in pancreatic acinar cells. J Biol Chem. 2010; 285:38251–38259. [PubMed: 20870729]
23. Collins TP, Bayliss R, Churchill GC, Galione A, Terrar DA. NAADP influences excitation–contraction coupling by releasing calcium from lysosomes in atrial myocytes. Cell Calcium. 2011; 50:449–458. [PubMed: 21906808]
24. Oliver AE, Deamer DW. Alpha-helical hydrophobic polypeptides form proton-selective channels in lipid bilayers. Biophys J. 1994; 66:1364–1379. [PubMed: 7520289]
25. Vijayvergiya V, Wilson R, Chorak A, Gao PF, Cross TA, Busath DD. Proton Conductance of Influenza Virus M2 Protein in Planar Lipid Bilayers. Biophys J. 2004; 87:1697–1704. [PubMed: 15345548]
26. Koivusalo M, Steinberg BE, Mason D, Grinstein S. In situ Measurement of the Electrical Potential Across the Lysosomal Membrane Using FRET. Traffic. 2011; 12:972–982. [PubMed: 21554506]
27. Lloyd-Evans E, Morgan AJ, He XX, Smith DA, Elliot-Smith E, Sillence DJ, Churchill GC, Schuchman EH, Galione A, Platt FM. Niemann-Pick disease type C1 is a sphingosine storage disease that causes deregulation of lysosomal calcium. Nat Med. 2008; 14:1247–1255. [PubMed: 18953351]

28. Gerasimenko JV, Tepikin AV, Petersen OH, Gerasimenko OV. Calcium uptake via endocytosis with rapid release from acidifying endosomes. Curr Biol. 1998; 8:1335–1338. [PubMed: 9843688]
29. Steinberg BE, Huynh KK, Brodovitch A, Jabs S, Stauber T, Jentsch TJ, Grinstein S. A cation counterflux supports lysosomal acidification. J Cell Biol. 2010; 189:1171–1186. [PubMed: 20566682]
30. Grabe M, Oster G. Regulation of Organelle Acidity. J Gen Physiol. 2001; 117:329–344. [PubMed: 11279253]
31. Morgan AJ, Davis LC, Wagner SKTY, Lewis AM, Parrington J, Churchill GC, Galione A. Bidirectional Ca^{2+} signaling occurs between the endoplasmic reticulum and acidic organelles. J Cell Biol. 2013; 200:789–805. [PubMed: 23479744]
32. Lu Y-Y, Hao B-X, Graeff R, Wong CWM, Wu W-T, Yue J. TPC2 Signaling Inhibits Autophagosomal-Lysosomal Fusion by Alkalizing Lysosomal pH. J Biol Chem. 2013; 288:24247–24263. [PubMed: 23836916]
33. Liu W, Pasek DA, Meissner G. Modulation of Ca^{2+} -gated cardiac muscle Ca^{2+} -release channel (ryanodine receptor) by mono- and divalent ions. Am J Physiol. 1998; 274:C120–C128. [PubMed: 9458720]
34. Richard E, Miller C. Steady-state coupling of ion-channel conformations to a transmembrane ion gradient. Science. 1990; 247:1208–1210. [PubMed: 2156338]
35. Van Helden DF, Hamill OP, Gage PW. Permeant cations alter endplate channel characteristics. Nature. 1977; 269:711–713. [PubMed: 413051]
36. Moroni M, Biro I, Giugliano M, Vijayan R, Biggin PC, Beato M, Sivilotti LG. Chloride Ions in the Pore of Glycine and GABA Channels Shape the Time Course and Voltage Dependence of Agonist Currents. J Neurosci. 2011; 31:14095–14106. [PubMed: 21976494]
37. Holmgren M. Influence of Permeant Ions on Gating in Cyclic Nucleotide–gated Channels. J Gen Physiol. 2003; 121:61–72. [PubMed: 12508054]
38. Pitt SJ, Funnell TM, Zhu MX, Parrington J, Ruas M, Galione A, Sitsapesan R. TPC2 is a Novel NAADP-Sensitive Intracellular Ca^{2+}-Release Channel with Unique Gating Characteristics. Biophys J. 2011; 100:433a.
39. Ward JM, Schroeder JI. Calcium-Activated K^+ Channels and Calcium-Induced Calcium Release by Slow Vacuolar Ion Channels in Guard Cell Vacuoles Implicated in the Control of Stomatal Closure. The Plant Cell Online. 1994; 6:669–683.
40. Furuichi T, Cunningham KW, Muto S. A Putative Two Pore Channel AtTPC1 Mediates Ca^{2+} Flux in Arabidopsis Leaf Cells. Plant Cell Physiol. 2001; 42:900–905. [PubMed: 11577183]
41. Jiang Y-L, Lin AHY, Xia Y, Lee S, Paudel O, Sun H, Yang X-R, Ran P, Sham JSK. Nicotinic Acid Adenine Dinucleotide Phosphate (NAADP) Activates Global and Heterogeneous Local Ca^{2+} Signals from NAADP- and Ryanodine Receptor-gated Ca^{2+} Stores in Pulmonary Arterial Myocytes. J Biol Chem. 2013; 288:10381–10394. [PubMed: 23443655]
42. Ogunbayo OA, Zhu Y, Rossi D, Sorrentino V, Ma J, Zhu MX, Evans AM. Cyclic Adenosine Diphosphate Ribose Activates Ryanodine Receptors, whereas NAADP Activates Two-pore Domain Channels. J Biol Chem. 2011; 286:9136–9140. [PubMed: 21216967]
43. Tugba Durlu-Kandilci N, Ruas M, Chuang KT, Brading A, Parrington J, Galione A. TPC2 Proteins Mediate Nicotinic Acid Adenine Dinucleotide Phosphate (NAADP)- and Agonist-evoked Contractions of Smooth Muscle. J Biol Chem. 2010; 285:24925–24932. [PubMed: 20547763]
44. Churamani D, Hooper R, Rahman T, Brailoiu E, Patel S. The N-terminal region of two-pore channel 1 regulates trafficking and activation by NAADP. Biochem J. 2013; 453:147–151. [PubMed: 23634879]
45. Carrithers MD, Dib-Hajj S, Carrithers LM, Tokmoulina G, Pypaert M, Jonas EA, Waxman SG. Expression of the Voltage-Gated Sodium Channel NaV1.5 in the Macrophage Late Endosome Regulates Endosomal Acidification. The Journal of Immunology. 2007; 178:7822–7832. [PubMed: 17548620]
46. Dong, X-p; Shen, D; Wang, X; Dawson, T; Li, X; Zhang, Q; Cheng, X; Zhang, Y; Weisman, LS; Delling, M; Xu, H. PI(3,5)P2 controls membrane trafficking by direct activation of mucolipin Ca^{2+} release channels in the endolysosome. Nat Commun. 2010; 1:38. [PubMed: 20802798]

47. Harikumar P, Reeves JP. The lysosomal proton pump is electrogenic. J Biol Chem. 1983; 258:10403–10410. [PubMed: 6224789]
48. Jha A, Ahuja M, Patel S, Brailoiu E, Muallem S. Convergent regulation of the lysosomal two-pore channel-2 by Mg^{2+}, NAADP, PI(3,5)P2 and multiple protein kinases. The EMBO Journal. 2014; 33:501–511. [PubMed: 24502975]
49. Sitsapesan R, Montgomery RAP, MacLeod KT, Williams AJ. Sheep cardiac sarcoplasmic reticulum calcium release channels: modification of conductance and gating by temperature. J Physiol. 1991; 434:469–488. [PubMed: 1850797]
50. Colquhoun, D, Sigworth, FJ. Single-channel recording. Sakmann, B, Neher, E, editors. Vol. 1. Plenum; New York & London: 1983. 191–263.
51. Hodgkin AL, Katz B. The effect of sodium ions on the electrical activity of the giant axon of the squid. J Physiol. 1949; 108:37–77. [PubMed: 18128147]
52. Fatt P, Ginsborg BL. The ionic requirements for the production of action potentials in crustacean muscle fibres. J Physiol. 1958; 142:516–543. [PubMed: 13576452]
53. Aarhus R, Graeff RM, Dickey DM, Walseth TF, Lee HC. ADP-ribosyl cyclase and CD38 catalyze the synthesis of a calcium-mobilizing metabolite from $NADP^+$ J Biol Chem. 1995; 270:30327–30333. [PubMed: 8530456]

Europe PMC Funders Author Manuscripts

Europe PMC Funders Author Manuscripts

One-sentence summary

Stimuli that increase calcium or NAADP may promote proton release from the endosomes and lysosomes by activating TPC1.

Europe PMC Funders Author Manuscripts

Editor's summary

Showing a Preference for Protons

Protons (H^+) and calcium (Ca^{2+}) produce a variety of different effects in cells. One way to determine which channels allow each of these ions to pass is to isolate the proteins and incorporate them into artificial bilayers. With this approach, Pitt *et al.* found that H^+ was the preferred ion that passed through the human two-pore channel 1 (TPC1), which in cells is located in acidic membrane-bound compartments called endosomes and lysosomes. They also identified intracellular signaling messengers that stimulated TPC1 and signals that changed the relative ability of different positively charged ions to flow through the channel. The exact function of the released H^+ remains an open question.

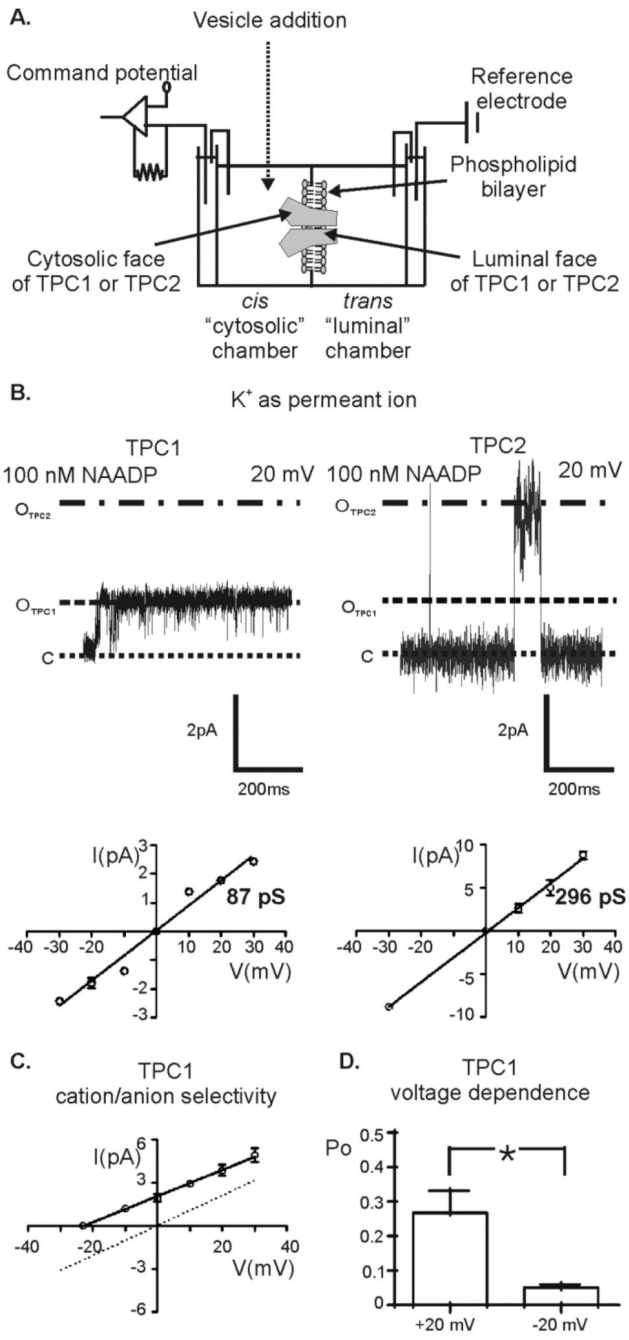

Figure 1. Single-channel properties of purified human TPC1 and TPC2 with K^+ as the permeant ion.

(A) A schematic diagram of the in-vitro bilayer system. The *trans* chamber was held at 0 mV and the *cis* chamber was voltage clamped at various potentials relative to ground. Under these conditions, with an open channel, cationic current will flow in the *trans* to *cis* direction at negative holding potentials and in the *cis* to *trans* direction at positive holding potentials. Vesicles were added to the *cis* chamber and after fusion with the bilayer, the orientation of TPC1 and TPC2 in the bilayer appeared to be consisten with the cytosolic side of TPC1 and

TPC2 facing into the *cis* chamber and the intralysosomal (luminal) side of the channels facing into the *trans* chamber. Multiple channels were present in each bilayer preparation and therefore Po measurements reflect the average Po measured over 3 min of recording for each intervention (see methods). Example traces were selected from sections of trace in which only a single channel was gating. **(B)** Single-channel recordings from TPC1 (left) and TPC2 (right) using K^+ as permeant ion (symmetrical 210 mM KCl solution) in the presence of 100 nM NAADP (cytosolic chamber) at holding potential +20 mV. The traces in this figure are not representative of Po but are chosen to show current amplitudes clearly. The unitary current amplitudes at +20 mV for TPC1 ($_{OTPC1}$) and TPC2 (^{OTPC2}) are indicated on the respective trace. The dotted line labelled C, represents the closed channel state. The lower panels show the I/V relationship for TPC1 (left) and TPC2 (right) in symmetrical 210 mM KCl solution. Values are mean ± SEM (n=4). **(C)** The I/V relationship for TPC1 in a KCl gradient (210 mM KCl luminal-chamber: 510 mM KCl cytosolic-chamber; solid line and closed circles) reveals a single-channel conductance of 82 ± 5 pS (values are mean ± SEM; n=3). The I/V relationship for TPC1 in symmetrical 210 mM KCl solution (dotted line) is shown for comparison. (**D**) The mean Po of TPC1 at holding potentials of +20 mV and -20 mV. Values are mean ± SEM (n=4). A paired t-test was used to compare means ($p < 0.05$).

Europe PMC Funders Author Manuscripts

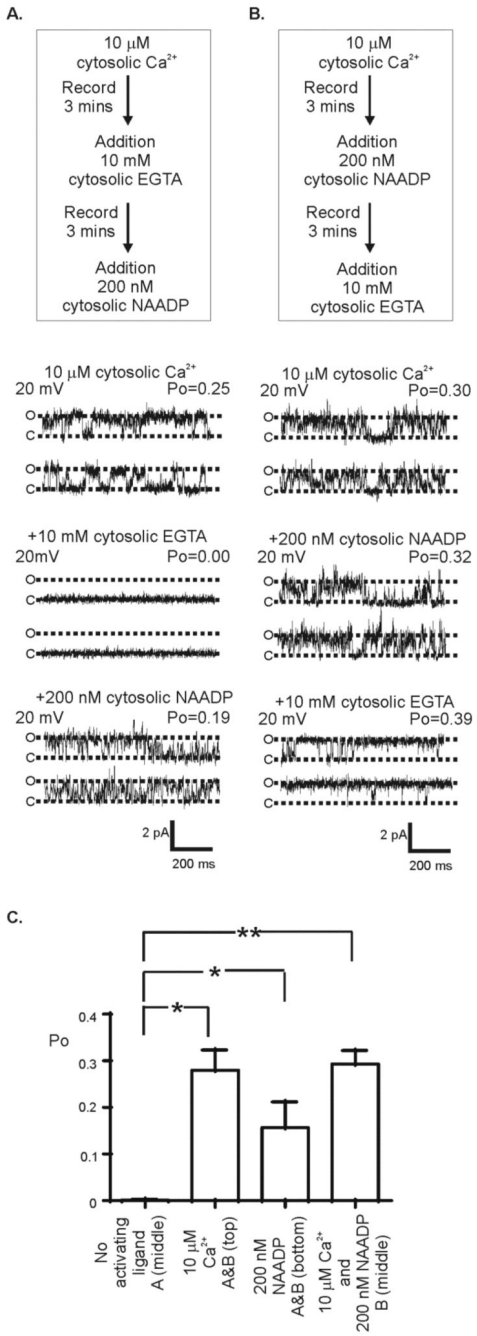

Figure 2. Effect of NAADP and cytosolic Ca^{2+} on TPC1 gating.

(**A**) Flow diagram detailing the experimental protocol with representative single-channel recordings shown below. TPC1 currents were recorded using K^+ as permeant ion (symmetrical 210 mM KCl solution) (top), following the addition of 10 mM EGTA (cytosolic chamber) to lower cytosolic [Ca^{2+}] to < 1 nM (middle), and after subsequent addition of 200 nM NAADP (cytosolic chamber) (bottom). (**B**) Flow diagram detailing the experimental protocol with representative single-channel recordings shown below. Current fluctuations show TPC1 activity with K^+ as permeant ion (symmetrical 210 mM KCl

solution) (top), after subsequent addition of 200 nM NAADP (cytosolic chamber) in the continued presence of 10 μM cytosolic Ca^{2+} (middle trace), and after subsequent addition of 10 mM EGTA (cytosolic chamber) to lower cytosolic [Ca^{2+}] to < 1 nM (bottom). The dotted lines indicate the (O) open and (C) closed state of the channel. (**C**) The mean Po from 6 individual single-channel experiments. Below each bar, reference to each treatment (as shown in A and B) is provided. In the absence of activating concentrations of Ca^{2+} and NAADP in the cytosolic chamber (no activating ligand) single channel activity is undetectable and Po=0. ANOVA followed by a modified *t*-test was used to assess the difference between treatments *=p<0.05, **=p<0.01). Values are mean ± SEM.

Europe PMC Funders Author Manuscripts

Europe PMC Funders Author Manuscripts

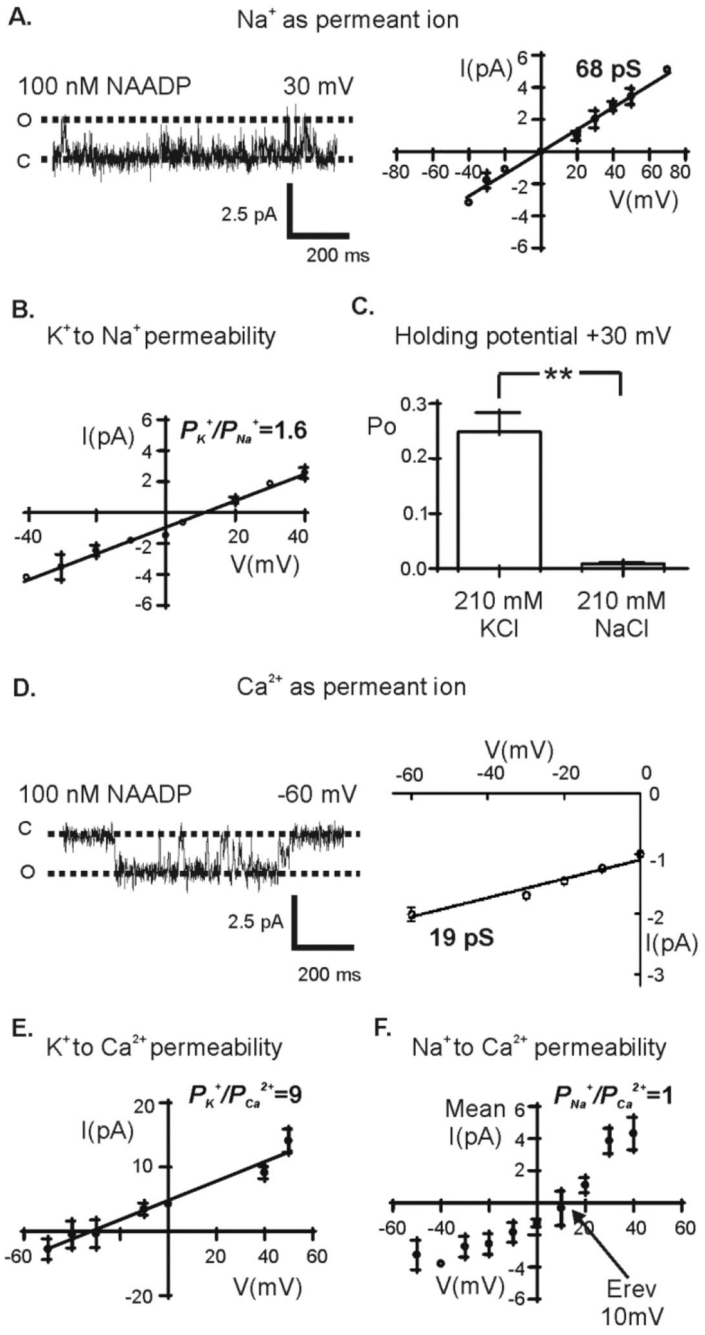

Figure 3. Ion permeation properties of TPC1.

(A) Single TPC1 current fluctuations and I/V relationship for TPC1 with Na^+ as the permeant ion (symmetrical 210 mM NaCl solution). The dotted lines indicate the (O) open and (C) closed channel state. **(B)** The relative K^+ to Na^+ permeability (P_{K^+}/P_{Na^+}) was calculated by construction of an I/V relationship with 210 mM KCl in the luminal chamber and 210 mM NaCl in the cytosolic chamber (n=6). **(C)** The mean Po from 6 paired experiments at holding potential +30 mV using either symmetrical 210 mM KCl solution or 210 mM NaCl solution. A paired t-test was used to compare means ($p < 0.01$). Values are

mean ± SEM. **(D)** Single-channel current fluctuations and the respective I/V relationship with Ca^{2+} as the permeant ion (Tris/HEPES:Ca^{2+}glutamate solutions). The relative K^+ to Ca^{2+} permeability ($P_{K^+}/P_{Ca^{2+}}$) **(E)** and the relative Na^+ to Ca^{2+} permeability ($P_{Na^+}/P_{Ca^{2+}}$) **(F)** was calculated by construction of an I/V relationship with either 210 mM KCl (n=5) or 210 mM NaCl (n=7) in the cytosolic chamber and 210 mM $CaCl_2$ in the luminal chamber. Values are mean ± SEM. The reversal potential (E_{rev}) is indicated.

Europe PMC Funders Author Manuscripts

Europe PMC Funders Author Manuscripts

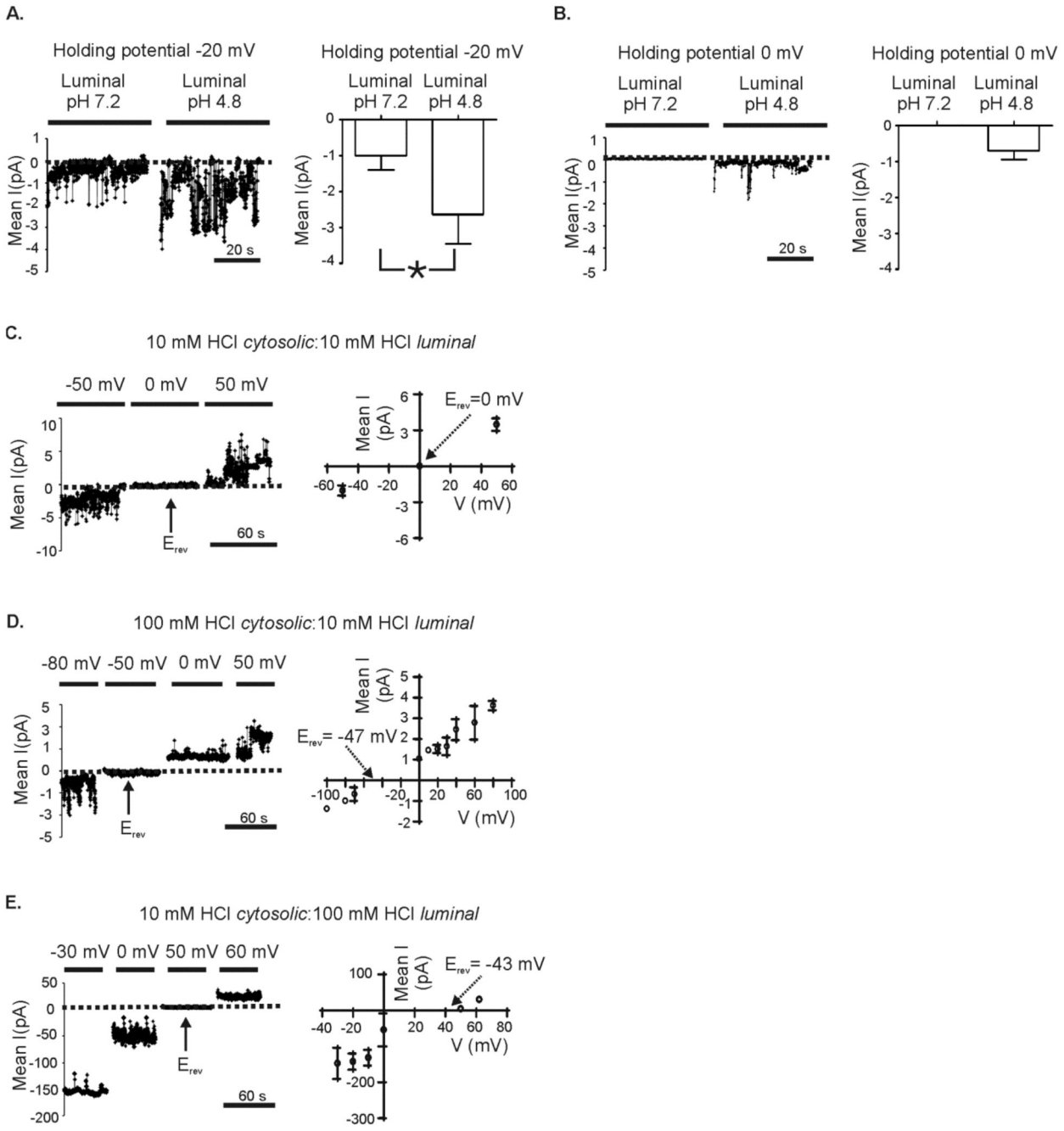

Figure 4. Effect of luminal pH on TPC1 gating.

Many channels were incorporated into the bilayer and the mean current was measured under the specified condition. Noise analysis of current fluctuations at -20 mV **(A)** and 0 mV **(B)** are shown using symmetrical 210 mM K^+-acetate solutions. In (A) and (B) the pH of the solution in the cytosolic chamber was maintained at 7.2 and the pH of the solution in the luminal chamber is as indicated. The dotted line in each current trace shows the zero current level. The corresponding bar charts show the mean current from 4 paired experiments. Values are means ± SEM. A paired *t*-test was used to compare means (* = $p < 0.05$). **(C-E)**

Noise analysis of current fluctuations at the indicated holding potential: (C) symmetrical pH 2, (D) pH 2 cytosolic chamber: pH 1 luminal chamber and (E) pH 1 cytosolic chamber: pH 2 luminal chamber. The current-voltage relationships to the right of the example traces show the mean data ± SEM obtained from 3-5 independent single-channel experiments. The arrows indicate the position of the reversal potentials.

Europe PMC Funders Author Manuscripts

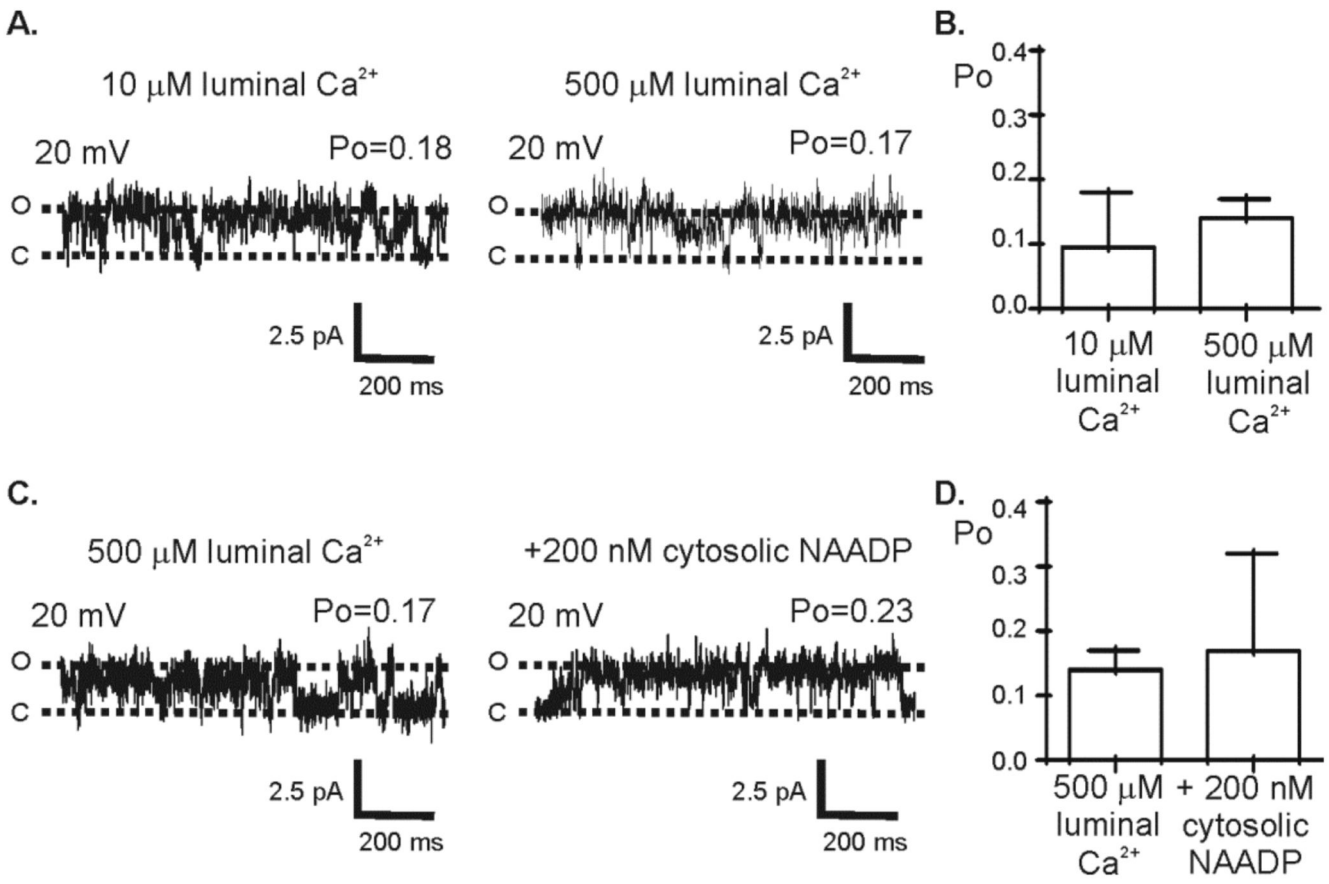

Figure 5. Effect of luminal Ca^{2+} on TPC1 gating.

(A) Representative TPC1 single-channel fluctuations following activation by 10 μM cytosolic Ca^{2+} with K^+ as the permeant ion (symmetrical 210 mM KCl solution) (left) and following the addition of 500 μM $CaCl_2$ to the luminal chamber (right). **(B)** Mean Po from 3 independent experiments carried out in an identical manner to the experiment shown in A. **(C)** A representative trace of TPC1 single-channel fluctuations with 500 μM Ca^{2+} (luminal chamber) in the absence (left) or presence (right) of 200 nM NAADP (cytosolic chamber). In (A) and (C), the dotted lines indicate the open (O) and closed (C) channel levels. **(D)** Mean Po in the presence or absence of NAADP when luminal side [Ca^{2+}] is 500 μM. Values are mean ± SEM (n=3).

Europe PMC Funders Author Manuscripts

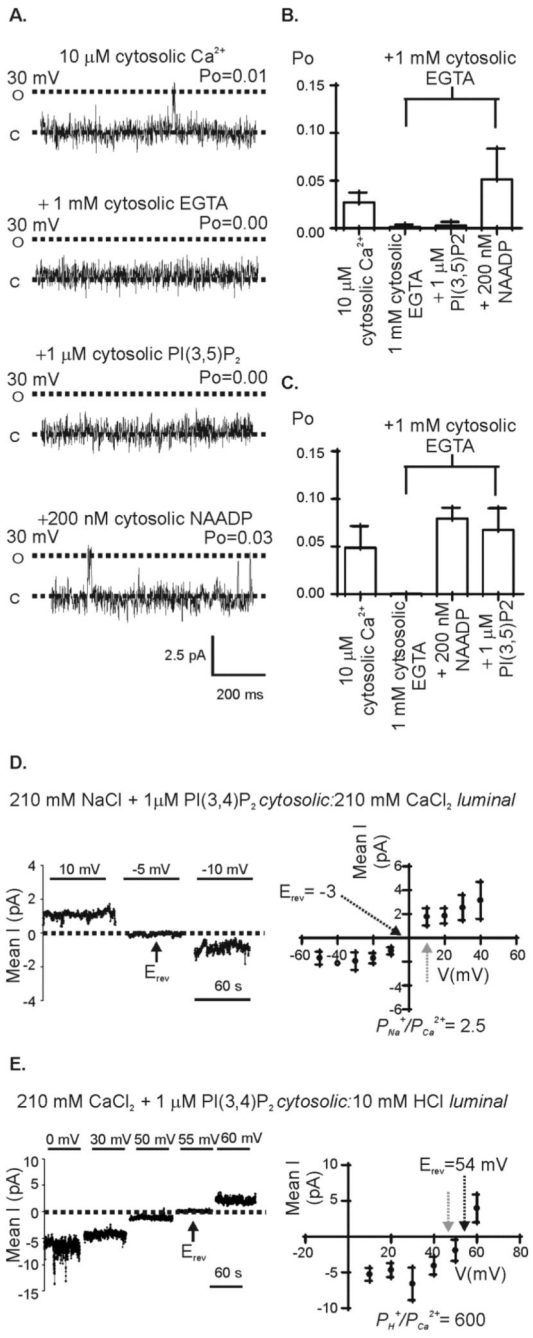

Figure 6. Effect of PI(3,5)P_2 on TPC1 gating.

(A) Representative single-channel current fluctuations using Na^+ as the permeant ion (symmetrical 210 mM NaCl solution), at +30 mV, followed by addition of 1 mM EGTA to the cytosolic chamber, followed by the addition of 1μM PI(3,5)P_2 to the cytosolic chamber, followed by the addition of 200 nM NAADP to the cytosolic chamber. **(B)** The mean channel Po from 4 independent experiments carried out in an identical manner to the experiment shown in A. **(C)** The mean channel Po from 3 independent experiments using Na^+ as the permeant ion (symmetrical 210 mM NaCl solution) at a holding potential +30 mV,

when the order of addition was addition of 1 mM EGTA to the cytosolic chamber, followed by the addition of 200 nM NAADP (cytosolic chamber), and then the addition of 1 μM $PI(3,5)P_2$ (cytosolic chamber). In the presence of 1 mM EGTA, cytosolic [Ca^{2+}] is insufficient to activate the channel. **(D, E)** Effect of $PI(3,5)P_2$ on the relative permeabilities to Na^+ (D) and H^+ (E) compared to Ca^{2+}. Multiple TPC1 channels were incorporated into each bilayer and the mean current was measured at the indicated holding potential in the presence of 1 μM $PI(3,5)P_2$ (cytosolic chamber) with the indicated ionic solutions in the cytosolic and luminal chambers. The current fluctuations on the left show typical examples of the noise analysis calculated at the indicated holding potentials. The dotted line shows the zero current level. The I/V relationships to the right of the example traces show the mean data from 4-6 independent experiments. The black arrows indicate the position of the reversal potentials. For comparison, the measured reversal potential obtained from the same paired experiment in the absence of $PI(3,5)P_2$ is shown on the I/V relationship as a dotted grey arrow.

Europe PMC Funders Author Manuscripts

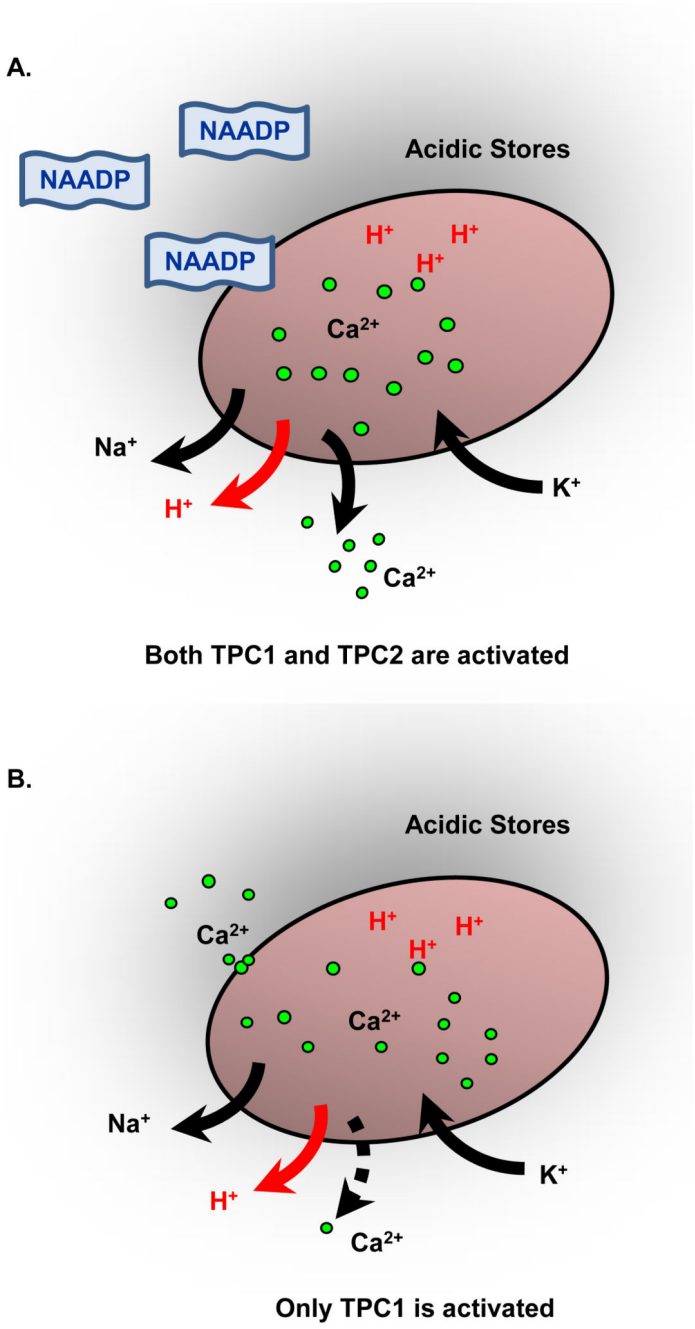

Figure 7. Model of lysosomal ionic currents that flux through TPCs following activation by NAADP or Ca^{2+}.

(A) The effects of NAADP. Both TPC1 and TPC2 will be activated. Na^+ will flow outwards through both TPC1 and TPC2. Ca^{2+} will flow outwards primarily through TPC2 and H^+through TPC1 only. **(B)** The effects of an increase in cytosolic Ca^{2+}. Only TPC1 will be activated and only a very small amount of Ca^{2+} will be released with H^+ from lysosomal stores.

Europe PMC Funders Author Manuscripts

Table 1

Basic biophysical properties of TPC1.

When K^+ or Na^+ was permeant ion, the cytosolic and luminal chambers contained symmetrical solutions of either 210 mM KCl or 210 mM NaCl. When Ca^{2+} was permeant ion, Tris/HEPES: Ca^{2+}glutamate solutions were used (full details of solutions described in Materials and Methods). The holding potential is shown in mV. For measurements of Po in which NAADP was the sole activating ligand, 10 mM EGTA was first added to the cytosolic chamber to lower the [Ca^{2+}] to subactivating concentrations prior to the addition of 100 nM NAADP. Values are mean ± SEM.

			10 μM cytosolic Ca^{2+} as activating ligand			100 nM NAADP as activating ligand		
Permeant ion	**Single-channel conductance (pS)**	***n***	**Po**	**mV**	***n***	**Po**	**mV**	***n***
K^+	87 ± 3	4	0.26± 0.06	20	5	0.17± 0.04	20	5
Na^+	68 ± 3	5	0.05± 0.01	30	8	0.08± 0.006	30	4
Ca^{2+}	19 ± 2	3	0.1± 0.08	-60	3	-		

Table 2

Permeability properties of TPC1.

Relative permeability ratios were calculated from measurements made under bi-ionic conditions. TPC1 permeability of Na^+ and H^+ relative to Ca^{2+} following the addition of 1 μM $PI(3,5)P_2$ to the cytosolic chamber is also shown. The solutions used were 210 mM $CaCl_2$ solution, 210 mM KCl solution, 210 mM NaCl solution, 10 mM HCl (pH 2) as described in Materials and Methods. A paired *t*-test was used to assess the difference between mean values. Values are mean ± SEM.

Permeability difference between Na^+ and Ca^{2+}, H^+ or K^+					
Ion	P_x^+/P_{Na}^+	*n*	P_x^+/P_H^+	*n*	
Ca^{2+}	0.98 ± 0.1	7	0.002 ± 0.0001	6	
H^+	66.8 ± 15	5	-		
K^+	1.6 ± 0.08	6	0.03 ± 0.01	3	
Na^+	-	-	0.015 ± 0.004	5	
Permeability difference between Ca2$^+$ Na^+, H^+ or K^+					
			Addition of 1 μM $PI(3,5)P_2$		
Ion	P_x^+/P_{Ca}^{2+}	*n*	p_x^+/P_{ca}^{2+}	*n*	*p* value (paired *t* test)
Na^+	1.1 ± 0.11	7	2.4 ± 0.06	4	0.05
H^+	503 ± 35	6	585 ± 34	6	0.001
K^+	9 ± 2.4	5	-		